

# FORMATION OF TURBULENT CONES IN ACCRETION DISK OUTFLOWS AND APPLICATION TO BROAD LINE REGIONS OF ACTIVE GALACTIC NUCLEI

A. Y. POLUDNENKO<sup>1</sup>, E. G. BLACKMAN<sup>2</sup>, A. FRANK<sup>3</sup>

Department of Physics and Astronomy,  
University of Rochester, Rochester, NY 14627-0171  
*Submitted to the Astrophysical Journal Letters*

## ABSTRACT

We consider the stability of an accretion disk wind to cloud formation when subject to a central radiation force. For a vertical launch velocity profile that is Keplerian or flatter and the presence of a significant radiation pressure, the wind flow streamlines cross in a conical layer. We argue that such regions are highly unstable, and are natural sites for supersonic turbulence and, consequently, density compressions. We suggest that combined with thermal instability these will all conspire to produce clouds. Such clouds can exist in dynamical equilibrium, constantly dissipating and reforming. As long as there is an inner truncation radius to the wind, our model emerges with a biconical structure similar to that inferred by Elvis (2000) for the broad line region (BLR) of active galactic nuclei (AGN). Our results may also apply to other disk-wind systems.

*Subject headings:* hydrodynamics — instabilities — turbulence — galaxies:active — (galaxies:) quasars: emission lines — galaxies: Seyfert — (galaxies:) cooling flows

## 1. INTRODUCTION

Non-spherical outflows are a ubiquitous feature of AGN. In this Letter we discuss the stability of such an outflow launched normally from the disk with a decaying power law velocity profile. The motivation for this work is to understand the conditions under which the flow may be unstable to cloud formation, and to infer the structure of the region in which such clouds may reside. Elvis (2000) has argued that data require AGN BLR clouds to reside in a narrow biconical structure. Our work herein supports this possibility.

A variety of launching mechanisms for AGN accretion disk outflows have been studied: radiatively accelerated outflows (Arav *et al.* 1994), hydrodynamic line-driven winds (Proga *et al.* 1999, 2000), hydromagnetic disk winds (Königl & Kartje 1994), (Pelletier & Pudritz 1992), thermal wind-type outflows in low luminosity AGNs (Pietrini & Torricelli-Ciamponi 2000), and others. In this work we parameterize the disk wind independent of the launching mechanism.

A disk wind outflow can become unstable from linear and nonlinear perturbations in velocity, density, temperature, ionization state, etc. These can lead to cloud formation. The cloud model is a leading, though not unanimously accepted, paradigm for the structure of the AGN BLR regions: models exist with (Elvis 2000; Urry & Padovani 1995) and without (Murray & Chiang 1995; Murray *et al.* 1995) clouds. The main reason for the lack of agreement is the uncertainty about cloud survival in AGN environments (Mathews & Ferland 1987). They may be unstable to evaporation (e.g., see (Pier & Voit 1995)), or be insufficiently supported by pressure and be dynamically unstable to shredding (Mathews & Ferland 1987; Poludnenko *et al.* 2002). Among the suggested solutions has been magnetic confinement of clouds (Rees 1987; Bottorff & Ferland 2000).

However a key point is that a typical cloud needs only to exist long enough to reprocess radiation (Rees 1987; Celotti *et al.* 1992; Kuncic *et al.* 1996, 1997). If clouds are destroyed thereafter and new clouds are formed, then the system can exist in

dynamical equilibrium even though each cloud loses its identity swiftly. This may apply to the broad line region. Short cloud survival and regeneration times can be associated with turbulence (Bottorff & Ferland 2001; Bottorff *et al.* 2000). The balance between formation and destruction maintains a constant BLR cloud number density.

Our analysis suggests that a nonlinear wind instability resulting from the combination of launching profile + radiation pressure can lead to the formation of a turbulent biconical zone that might manifest itself observationally as the BLR. This biconical structure is the region where flow streamlines cross. Such a bicone is remarkably similar to that inferred empirically by Elvis (2000) and from numerical simulations by Proga *et al.* (2000). Growing observational data corroborates the existence of such a structure (e.g. NGC 1068 (Arribas *et al.* 1996), Mrk 3 (Ruiz *et al.* 2001), etc.)

We formulate the problem in section 2.1 and describe the flow field in section 2.2. We analyze the linear and nonlinear stability of the flow and a possible scenario for thermal instability resulting in formation of the BLR clouds in section 2.3. In section 3 we discuss the results and their implications for the AGN structure and dynamics.

## 2. DISK WIND MODEL

### 2.1. Formulation of the problem

All of our calculations are performed in cylindrically symmetric geometry, however we do not include axial rotation. At the origin we assume a black hole of mass  $M_{BH}$ . Fig. 1 shows the setup.

We take a Keplerian, geometrically thin, optically thick accretion disk to be located along the abscissae with the distance  $\lambda$  measured along the disk. The central engine is taken to be a point-like source at the origin coincident with the black hole. We exclude disk surface illumination by the central source including all disk properties into the disk-wind launch velocity profile.

<sup>1</sup> wma@pas.rochester.edu

<sup>2</sup> blackman@pas.rochester.edu

<sup>3</sup> afrank@pas.rochester.edu

Our wind originates at the disk surface with launch velocity profile

$$v_{z0}(\lambda) = v^* \left( \frac{\lambda}{\lambda^*} \right)^n, \quad (1)$$

where  $v^*$  is the wind velocity at the innermost launch point of the disk with coordinate  $\lambda^*$  and  $n$  is an arbitrary non-positive number<sup>4</sup>. We assume that the wind propagates into a low density medium.

After the wind material leaves the disk, it is subjected to gravity from the black hole and radiation from the central engine. Proga *et al.* (1999, 2000) discuss one possible approach to line driven winds in the context of numerical modeling. To capture the most important qualitative features of the flow and to simplify the analysis we assume a continuum driven wind and use only Thomson opacities. This assumption somewhat underestimates the driving force since it excludes the contribution of line-driving. However, on the other hand, it is an overestimate since typically a significant fraction of the central source spectrum lies in the Compton scattering regime. To compensate for that we introduce a factor  $f_T < 1$ , intended to decrease the total luminosity  $L$ . The choice of a specific value of  $f_T$  depends on a particular situation being considered.

In our model, a fluid parcel of density  $\rho$  leaves the disk with the velocity of equation (1), determined by the coordinate of its launch point, and finds itself in a centrally symmetric, conservative potential field. For Thomson scattering the radiative force per unit volume is

$$\vec{F}^{rad}(r) = \frac{1}{c} \frac{\vec{r}}{|\vec{r}|} \int \alpha_\nu F_\nu d\nu = \frac{n\sigma_{T,e}}{c} F \frac{\vec{r}}{|\vec{r}|}, \quad (2)$$

and the effective potential field is

$$U(r) = U_{rad} + U_{grav} = \frac{\rho G M_{BH}}{r} \left( \frac{f_T L}{L_{Edd}} - 1 \right) = \rho \frac{\alpha}{r}, \quad (3)$$

where  $L_{Edd} = 1.25 \cdot 10^{38} \text{ erg/s} (M_{BH}/M_\odot)$  is the Eddington luminosity. Note, that here we give an expression for the potential energy per unit volume.

## 2.2. Description of the flow field

Finding a trajectory and velocity of a fluid parcel in the outflow reduces to the problem of the motion of a particle in a centrally symmetric repulsive potential, described by (3). The trajectory is a hyperbola (Landau & Lifshitz 1976), and in polar coordinates is

$$r(\phi) = \frac{p}{e \cos \phi - 1}. \quad (4)$$

Here  $\phi \in [0, \pi/2]$ . Eccentricity of the orbit  $e$  and parameter of the orbit  $p$  are defined as

$$e = 1 + \frac{p}{r_0}, \quad p = 2K \left( \frac{r_0}{r^*} \right)^{2n+1} r_0, \quad (5)$$

where  $r_0 = \lambda_0$  is the coordinate of the fluid element launch point. The dimensionless quantity

$$K = \lambda^* (v^*)^2 / 2\alpha, \quad (6)$$

is the ratio of the initial kinetic energy of a fluid particle launched at  $\lambda^*$  to its potential energy and measures the relative importance of the disk wind vs. central radiation source. ( $K$  and  $n$  are the key parameters in our analysis). Equation (4) can be considered as an implicit solution for  $\lambda_0$  as a function of  $z$  and

<sup>4</sup> We discard positive values of  $n$  as unphysical.

$\lambda$ . For any point  $(\lambda, z)$  we can uniquely determine the launch point of the streamline,  $\lambda_0$ . Fig. 1 shows a sample streamline pattern.

The velocity distribution along a streamline is

$$\begin{cases} v_\lambda(\lambda_0, \lambda) = \sqrt{\frac{\alpha}{\lambda_0} (e+1) \frac{\sinh \xi}{e \cosh \xi + 1}}, \\ v_z(\lambda_0, \lambda) = \sqrt{\frac{\alpha}{\lambda_0} (e^2 - 1)(e+1) \frac{\cosh \xi}{e \cosh \xi + 1}}. \end{cases} \quad (7)$$

Parameter  $\xi \in [0, +\infty)$  is defined by  $\cosh \xi = (\lambda/\lambda_0)(e+1) - e$ .

## 2.3. Stability analysis

We base our linear stability analysis for the inviscid case on the *Fjortoft theorem*, which is derived from the inviscid limit of the Orr-Sommerfeld equation, i.e. Rayleigh equation (Yih 1969; Maslowe 1985). We have studied the outflows with the values of  $-2.5 \leq n \leq 0.0$  and  $0.05 \leq K \leq 2.5$ . In all the regimes studied, the disk wind is linearly stable to infinitesimal velocity perturbations.

However a study of equation (4) shows that a non-linear instability can be present in a subregion of the flow. Depending on  $n$ , a streamline inclination angle at any given point  $(r, \lambda)$  is either a monotonically increasing or monotonically decreasing function of  $\lambda_0$ . The condition for the change in the character of monotonicity can be obtained: using equation (4) we can determine the inclination angle of a given streamline  $\tan \Theta(\lambda_0, \lambda) = dz/d\lambda$ . Using

$$\frac{d}{d\lambda_0} \left( \lim_{\lambda \rightarrow \infty} \tan \Theta(\lambda_0, \lambda) \right) = 0, \quad (8)$$

we find that the monotonicity changes for  $n = -1/2$ , i.e. the Keplerian disk is the borderline case. This means that for  $n > -1/2$ , each successive streamline is less inclined towards the abscissae axis than the preceding one and eventually intersects all of the preceding streamlines. For  $n \leq -1/2$  the inclination angle is a monotonically non-increasing function of  $\lambda_0$  and then the streamlines never intersect.

The intersection of two streamlines can be approximated as an intersection of two jets of vanishing thickness whose interaction leads to a resultant turbulent jet with an inclination angle lying between that of the two original jets (e.g., see (Landau & Lifshitz 1959)). Therefore, streamline intersection causes the biconical zone of compressible turbulence in the overall disk-wind outflow. The extent of such a zone can be estimated: since the streamline inclination angle is a monotonically increasing function of  $\lambda_0$ , the streamline originating at the innermost radius of the disk is the most inclined one. Therefore, it delineates the lower boundary of the turbulent biconical zone. Its inclination angle is

$$\tan \Theta_{min} = \lim_{\lambda \rightarrow \infty} \frac{dz}{d\lambda}(\lambda^*, \lambda) = 2\sqrt{K + K^2}. \quad (9)$$

An exact shape of the upper boundary of the bicone can be found by solving  $dz/d\lambda_0 = 0$  for  $\lambda_0$  as a function of  $\lambda$  and then substituting it into the equation (4) to find the exact dependence  $z(\lambda)$  for the upper boundary. Instead, we give an approximate expression for the inclination angle of the outer boundary, found by analogy to equation (9):

$$\begin{aligned} \tan \Theta_{max} &= \lim_{\lambda \rightarrow \infty} \frac{dz}{d\lambda}(\lambda_0, \lambda) \\ &= 2\sqrt{K \left( \frac{\lambda_0}{\lambda^*} \right)^{2n+1} + K^2 \left( \frac{\lambda_0}{\lambda^*} \right)^{2(2n+1)}}. \end{aligned} \quad (10)$$

This defines the basic geometry of the bicone: the *inclination angle*  $\Theta = (\Theta_{\max} + \Theta_{\min})/2$  and the *divergence angle*  $\Delta\Theta = \Theta_{\max} - \Theta_{\min}$ . See Figure 1.

Typically, the bicone has a divergence angle  $\Delta\Theta$  that slowly increases with radius. Therefore equation (10), which gives the limiting inclination angle of the streamline originating from the point  $\lambda_0$ , depends on the choice of such a particular streamline. However, the increase in the divergence angle is typically small. Moreover, a particular streamline used to determine  $\Theta_{\max}$  can be determined independently from the properties of the accretion disk or the estimated extent of the outflow.

Three other effects will enter in a more detailed hydrodynamic treatment that influence the divergence angle of the bicone. An effect which tends to make the divergence angle smaller than that determined using equations (9) and (10) arises because the resultant of two intersecting jets lies at an intermediate angle between the original two. Each successive interaction of resultant jets would then tend to narrow the overall conical structure. In addition, the change in the optical depth of the outflow after the formation of the turbulent bicone would shade the outer parts of the outflow. This will make the bicone narrower by increasing the inclination angle of the outer streamlines due to the reduced radiation pressure. In competition with both of these above effects is the turbulence itself, which could broaden the bicone.

The initial density fluctuations in the turbulent biconical zone cannot themselves represent the BELR clouds; the density and temperature contrasts are too small compared to the ambient warm highly ionized gas (WHIM in the nomenclature of Elvis (2000)). However, thermal instability in such a medium can transform initial turbulent overdensities into the BELR clouds (see (Burkert & Lin 2000; Hennebelle & Péroult 1999) for the discussion of two-phase medium formation via linear thermal instability in optically thin regions). The formation of the compressible turbulent bicone from intersecting flows can produce inhomogeneities with density contrast up to 4 in the adiabatic case and higher if one allows for the possibility of radiative cooling. Such high density contrasts (compared to the linear density fluctuations discussed by Burkert & Lin (2000)) can serve as a seed for thermal instability. The instability proceeds in the nonlinear regime from the onset. Rapid cooling would then produce clumps. The maximum clump density reached at a given scale is determined by how much cooling can occur during an eddy turnover time on that scale, i.e. during an average clump survival time.

This mechanism can lead to a dynamical equilibrium described by the balance between in situ formation, destruction, and re-formation of clumps comoving with the ambient flow. As long as any given clump survives long enough to reprocess radiation, problems of clump confinement against thermal conduction and destruction via high velocity differences between the clumps and the ambient medium are eliminated. The dynamical equilibrium of the turbulent flow, ensures a constant number density of BELR clouds in the turbulent biconical zone over observation durations.

Finally, there is a site where a linear instability of the Kelvin-Helmholtz type might operate, namely the shear layer between the disk wind outflow and the infalling (or stationary) circumpolar material, that fills the cone of the outflow. Simulations of Proga *et al.* (2000) show the formation of clumpy structure in that boundary shear layer. They attribute it to the Kelvin-

Helmholtz instability. However, in regimes for which the outflow develops the turbulent bicone, such linear instability will be completely overwhelmed by the nonlinear instability induced by the intersection of streamlines. In cases when the bicone is not formed, the outflow density decreases from the maximum values near the plane of the disk to nearly the values of the circumpolar infalling material in the upper parts of the outflow with the density transition occurring over the large range of angles. BLR clouds are not expected in this case.<sup>5</sup>

### 3. DISCUSSION

We considered the linear and nonlinear stability of a disk outflow and found that it is linearly stable to infinitesimal velocity perturbations. However, when  $n > -1/2$  and a supereddington radiation source is present, nonlinear instability leads to the formation of a biconical zone of compressible turbulence. High density contrasts in this zone may trigger thermal instability and lead to the further condensation of clumps into BELR clouds. Turbulence plays a key role in establishing the dynamical equilibrium which maintains a steady cloud number density, even though each cloud is short lived.

In the regimes when the outflow can develop the turbulent bicone, the geometry is remarkably similar to that described by Elvis (2000). For a disk outflow with  $K \approx 0.05$  and an initial launch velocity profile slightly flatter than Keplerian, namely  $n = -0.45$ , the turbulent bicone inclination angle is  $\Theta \approx 28^\circ$  with the divergence angle  $\Delta\Theta \approx 7^\circ$ . This is in quantitative and qualitative agreement with Elvis (2000): (1) no absorbers are along the line of sight passing above the outflow; (2) along the line of sight passing through the turbulent bicone broad absorption and emission line features will be observed; (3) narrow absorption lines (NAL) will be seen along sight lines that fall inside of the bicone. Figure 1 shows the geometry of the outflow and the emerging bicone with the angle values found here.

The outflow geometry in our picture depends only on dimensionless quantities  $K$  and  $n$ . However, in addition to  $\Theta$  and  $\Delta\Theta$  determined above, we can also infer the inner scale by matching observed cloud velocities. We assume the same value of  $n$  and  $K$  as in the previous paragraph. We take  $M_{BH} = 10^9 M_\odot$  and broad absorption line velocity  $v_{BAL} = 10^4 \text{ km s}^{-1}$  (the velocity observed when the line of sight passes directly along the bicone towards the central source). In our model  $v_{BAL}$  is the terminal velocity at infinity of material launched with the largest initial velocity and potential, i.e. at the point  $\lambda_0 = \lambda^*$ . Setting  $\lambda_0 = \lambda^*$  in (7) and using the expressions for  $v_\lambda(\lambda^*, \lambda)$  and  $v_z(\lambda^*, \lambda)$  in the limit  $\lambda \rightarrow \infty$ , we find

$$\lambda^* = \frac{2\alpha(1+K)}{v_{BAL}^2}. \quad (11)$$

Assuming  $L = 1.5L_{Edd}$  and  $f_T = 0.7$  the corresponding value of  $\lambda^* = \lambda_0 \approx 1000 \text{ a.u.}$ , which matches Elvis (2000). The corresponding maximum launch velocity is  $\approx 2000 \text{ km s}^{-1}$ . Therefore, the observed velocity in the NAL region is  $\sim 1000 \text{ km s}^{-1}$ .

In principle, the paradigm presented here applies not only to luminous AGN but to any source with a centrally symmetric potential, a sufficiently luminous central radiation source, and a disk wind, e.g. disk winds in young stellar objects.

We have not discussed the role of magnetic fields, disk rotation, metallicity, wind density fall off, or the physics of line driving. These should be considered in future work.

The authors thank V. Pariev for extremely important com-

<sup>5</sup> Note, that even in the cases when the turbulent bicone is absent the upper boundary of the outflow is still roughly defined by the streamline launched at  $\lambda^*$ .

ments and suggestions. AYP thanks N. Murray and M. Elvis for valuable discussions. AYP and AF acknowledge support from NSF grant AST-9702484 and NASA grant NAG5-8428. EGB

acknowledges support from DOE grant DE-FG02-00ER5460. The authors acknowledge DOE support from the Laboratory for Laser Energetics.

#### REFERENCES

- Arav, N., Li, Z.-Y., Begelman, M. C. 1994, *ApJ*, 432, 62  
 Arribas, S., Mediavilla, E., Garcia-Lorenzo, B. 1996, *ApJ*, 463, 509  
 Bottorff, M. C., Ferland, G. J. 2000, *MNRAS*, 316, 103  
 Bottorff, M. C., Ferland, G. 2001, *ApJ*, 549, 118  
 Bottorff, M., Ferland, G., Baldwin, J., Korista, K. 2000, *ApJ*, 542, 644  
 Burkert, A., Lin, D. N. C. 2000, *ApJ*, 537, 270  
 Celotti, A., Fabian, A. C., Rees, M. J. 1992, *MNRAS*, 255, 419  
 Elvis, M. 2000, *ApJ*, 545, 63  
 Hennebelle, P., Pérault, M. 1999, *A&A*, 351, 309  
 Königl, A., Kartje, J. F. 1994, *ApJ*, 434, 446  
 Kuncic, Z., Blackman, E. G., Rees, M. J. 1996, *MNRAS*, 283, 1322  
 Kuncic, Z., Celotti, A., Rees, M. J. 1997, *MNRAS*, 284, 717  
 Landau, L. D., Lifshitz, E. M. 1959, *Fluid Mechanics* (Reading : Addison-Wesley)  
 Landau, L. D., Lifshitz, E. M. 1976, *Mechanics* (Oxford, New York : Pergamon Press)  
 Maslowe, S. A. 1985, in *Hydrodynamic Instabilities and Transition to Turbulence*, ed. H.L. Swinney, J.P. Gollub (2nd ed.; Springer-Verlag), 181  
 Mathews, W. G., Ferland, G. J. 1987, *ApJ*, 323, 456  
 Murray, N., Chiang, J. 1995, *ApJ*, 454, L105  
 Murray, N., Chiang, J., Grossman, S. A., Voit, G. M. 1995, *ApJ*, 451, 498  
 Pelletier, G., Pudritz, R. E. 1992, *ApJ*, 394, 117  
 Pier, E. A., Voit, G. M. 1995, *ApJ*, 450, 628  
 Pietrini, P., Torricelli-Ciamponi, G. 2000, *ApJ*, 363, 455  
 Poludnenko, A. Y., Frank, A., Blackman, E. G. 2002, *ApJ*, in press  
 Proga, D., Stone, J. M., Drew, J. E. 1999, *MNRAS*, 310, 476  
 Proga, D., Stone, J. M., Kallman, T. R. 2000, *ApJ*, 543, 686  
 Ruiz, J. R., Crenshaw, D. M., Kraemer, S. B., Bower, G. A., Gull, T. R., Hutchings, J. B., Kaiser, M. E., Weistrop, D. preprint (astro-ph/0108521)  
 Rees, M. J. 1987, *MNRAS*, 228, 47p  
 Urry, C. M., Padovani, P. 1995, *PASP*, 107, 803  
 Yih, C. S. 1969, *Fluid Mechanics* (2d ed.; McGraw-Hill, New York 1969)

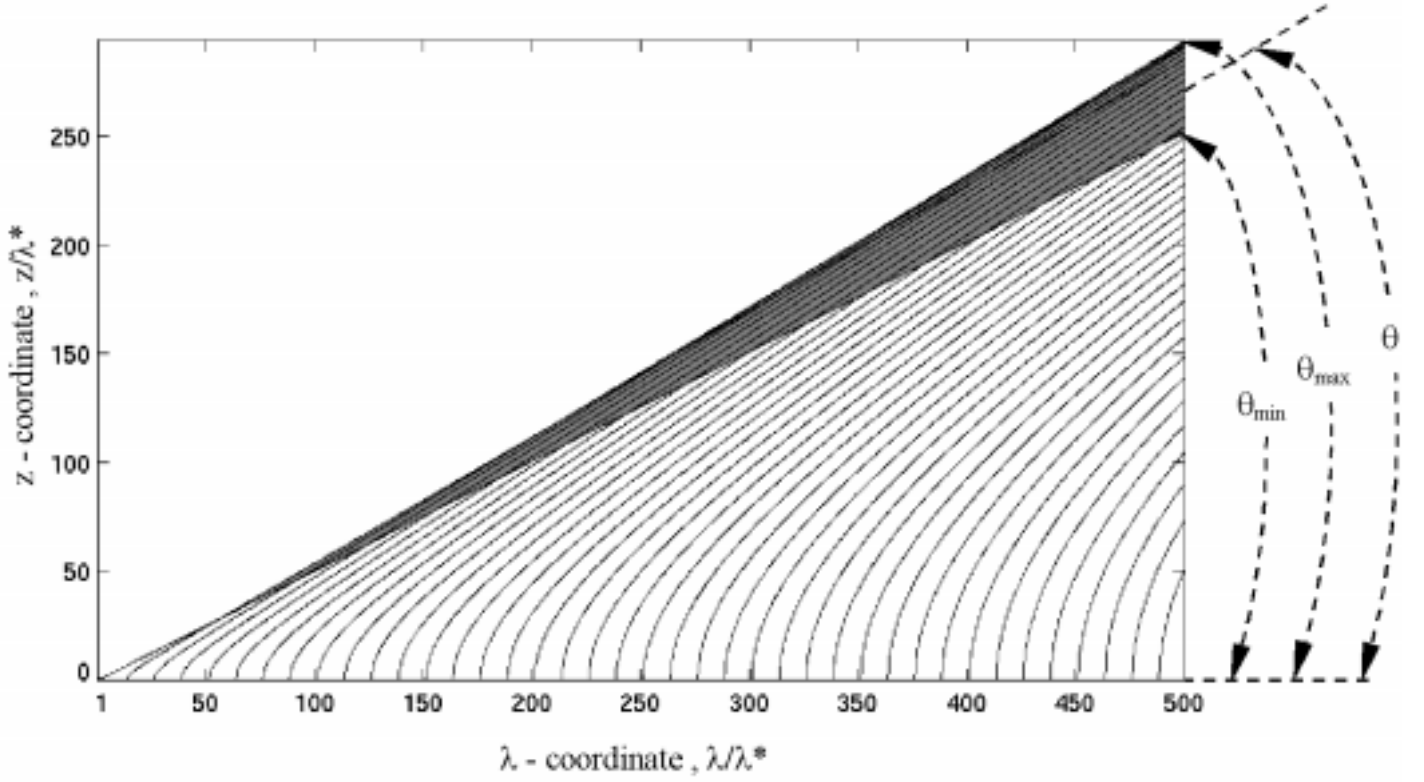


FIG. 1.— Sample streamline pattern for a disk wind outflow. Shown is the case  $n = -0.45$  and  $K = 0.06$ . Shaded region is the turbulent bicone formed by the intersection of streamlines. Values of the angles shown are discussed in the text.